AUTHORS	S. Sheludiakov, C. K. Wetzel, D. M. Lee, and V. V. Khmelenko, J. Järvinen, J. Ahokas, and S. Vasiliev
TITLE	Studies of accumulation rate of H atoms in solid H_2 films exposed to 0.1 and 5.7 keV electrons
YEAR	2023
DOI	https://doi.org/10.1103/PhysRevB.107.134110
VERSION	Author's accepted manuscript
CITATION	S. Sheludiakov, C. K. Wetzel, D. M. Lee, V. V. Khmelenko, J. Järvinen, J. Ahokas, and S. Vasiliev *Studies of accumulation rate of H atoms in solid H_2 films exposed to 0.1 and 5.7 keV electrons* Phys. Rev. B 107, 134110 – Published 17 April 2023

Studies of accumulation rate of H atoms in solid H_2 films exposed to 0.1 and 5.7 keV electrons

S. Sheludiakov
Department of Physics and Astronomy, University of Pittsburgh, Pittsburgh, PA, 15260, USA

C. K. Wetzel, D. M. Lee, and V. V. Khmelenko
Institute for Quantum Science and Engineering, Department of Physics and Astronomy, Texas A&M University, College Station, TX, 77843, USA

J. Järvinen,* J. Ahokas, and S. Vasiliev
Department of Physics and Astronomy, University of Turku, 20014 Turku, Finland
(Dated: April 6, 2023)

In this work, we report on Electron Spin Resonance studies of H atoms stabilized in solid H_2 films at temperature 0.1 and 0.7 K and in a magnetic field of 4.6 T. We produced H atoms by two different techniques: bombarding H_2 films by 0.1 keV electrons generated during an rf discharge run in the sample cell or exposing H_2 films to a flux of 5.7 keV electrons released during tritium decay. We observed a faster H atom accumulation in the films made of H_2 gas with a small initial ortho-H_2 content (0.2-3%) as compared with those made from the gas with a higher initial ortho-H_2 admixture. The accumulation rate difference was about 70% for the samples exposed to high energy electrons and about an order of magnitude for the samples bombarded by low-energy electrons. We propose possible explanations for the observed behavior.

I. INTRODUCTION

Hydrogen is the lightest and simplest among the elements. Along with solid helium and molecular hydrogen isotopes [1], hydrogen atoms embedded in solid H_2 represent a class of so-called quantum crystals, the only solid-state systems where atomic and molecular diffusion does not freeze even at temperatures below 1 K [2].

Hydrogen atoms are bosons and a possible observation of H atom Bose-Einstein Condensation (BEC) in a solid molecular hydrogen matrix constitutes an attractive goal for condensed matter research. For the realization of H atom BEC in a solid phase, the distance between hydrogen atoms should become comparable to their thermal de Broglie wavelength. To approach these extreme conditions, high concentrations of H atoms and their cooling to ultra-low temperatures are required. A thorough study of H atom accumulation in solid H_2 becomes particularly important for achieving high H atom concentrations.

Unlike He atoms, hydrogen atoms are unstable and tend to recombine back to molecules. They can, however, be stabilized in inert solid matrices of H_2 and noble gases by a number of techniques. Among them are a co-deposition of the rf discharge products onto a cold substrate [3, 4] or directly into superfluid He [5, 6] as well as co-deposition of the products of H-atom three-body recombination [7]. Another approach relies on bombardment of solid H_2 films by a flux of high-energy electrons [8–10], gamma-particles [11, 12], or photolysis of polar molecules such as HCl or HBr co-deposited with the inert matrix [13–16].

Exposure of solid H_2 to an electron beam primarily results in the formation of two H atoms for the electron energies up to 100 eV and H_2^+ ions at keV energies [17]. In the first case, the incident low-energy electrons excite H_2 molecules to the dissociation limit where they can split into two H atoms or they can gradually relax into the ground state through sequential de-excitation via a non-radiative multiphonon process with a rate $k_v \approx v \times 1.89 \times 10^5 \mathrm{s}^{-1}$, where v is the vibrational quantum number [18].

In the second case of high-energy electrons, the formed H_2^+ ions are not stable in the H_2 environment and convert into tri-hydrogen ions, H_3^+, via a chemical reaction $H_2^+ + H_2 = H_3^+ + H$. The tri-hydrogen ions can further react with electrons trapped in the lattice through the reaction $H_3^+ + e = H + H + H$ [17]. The observation of H_2^+ ions in solid neon by electron spin resonance (ESR) was reported by Correnti et al.[19], whereas H_3^+ ions have no electron spin and thus cannot be detected by ESR. These chemical reactions of simple hydrogen ions describe hydrogen dynamics in the primordial gas of the early Universe and play a special role in astrochemistry [20].

In a series of work, we studied H atoms in thin (0.1-2.5 μm) H_2 films of different ortho-para compositions. The H atoms were created by bombarding H_2 films with low-energy, $\simeq$100 eV, electrons while running the rf discharge above the H_2 films [2, 8, 21–23] or by exposing H_2 films to a flux of 5.7 keV electrons created during tritium decay [10, 24, 25]. In the former case, electrons can penetrate only into the 100 nm thick surface layer of the H_2 films. The atoms created there diffuse deeper into the film stimulated by a phonon flux from the discharge at the surface [2, 23]. High-energy electrons from the tritium decay penetrate through the whole film thickness and generate atoms evenly in the bulk of H_2 sample.

In the present work, we carry out an analysis of the

* Present address: Bluefors Oy, Arinatie 10, 00370 Helsinki, Finland

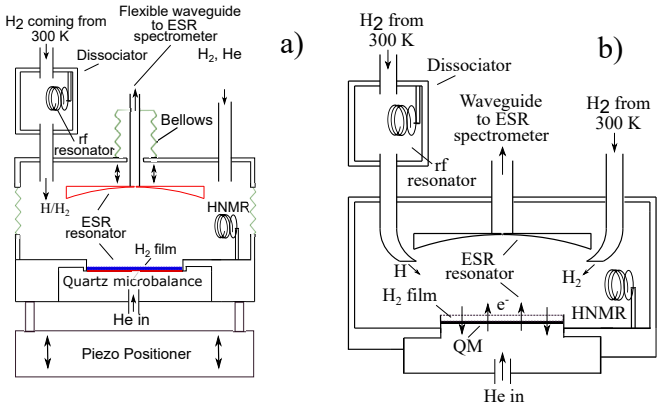

Figure 1. Schematic of sample cells used in experiments in Texas (a) and Turku (b). The helical resonators are labeled as HNMR.

H atom production rates in different H_2 samples studied in our previous and current work. We observed a higher accumulation rate of H atoms in H_2 samples with a small concentration of ortho-H_2 molecules (0.2-3% ortho-H_2) as compared with that in the H_2 films with a higher ortho-H_2 content. It also turned out that this difference was smaller for samples exposed to 5.7 keV electrons as compared to the films where H atoms were accumulated by running the rf discharge. We consider possible explanations for this phenomenon.

II. EXPERIMENTAL SETUP

The studies were carried out in two experimental setups located at the University of Turku and Texas A&M University. The setups are based on commercial dilution refrigerators: Oxford 2000 and Oxford 200, respectively. The sample cells (SC) of both setups are attached to the refrigerator mixing chambers and also located in the centers of 4.6 T superconducting magnets [26, 27]. The sample cells have similar designs as presented in Figs.1a and 1b. The main SC volumes contain open design ESR Fabry-Perot resonators coupled to 128 GHz ESR spectrometers [28] through a waveguide assembly. The top spherical ESR resonator mirrors of both SCs are made of polycrystalline copper, while the flat bottom metal-plated mirrors also correspond to the top electrode of a quartz microbalance (QM). The top mirror in the Texas setup was also plated with a μm-thick silver layer. The bottom flat mirrors in the Texas and Turku setups were Au and Pd-plated, respectively. We, therefore, simultaneously measured the H_2 film thickness by the QM and detected H atoms by means of ESR in both studies. We use the TX and TU notation for the samples studied at Texas A&M and the University of Turku, respectively.

The TX samples were created as follows. First, we deposited a 0.2-2.5 μm solid hydrogen film onto the QM top electrode by recondensing H_2 from a specially arranged chamber, the dissociator, which was thermally insulated from the SC body by a stainless steel tubing assembly. Prior to that, we had loaded a few mmoles of H_2 gas into this chamber. During the deposition process, the dissociator was heated to 5-7 K and the H_2 gas sublimated from its surfaces was directed into the SC and condensed on the QM surface. We deposited H_2 films with a typical rate of about 0.1-1 monolayer/s keeping the SC temperature stabilized at fixed temperature in the range T=0.5-1 K. In this regime, we were able to create uniform polycrystalline H_2 films with a low local inhomogeneity [26]. After that, we kept the SC temperature at T=0.7 K and condensed a few μmoles of helium gas there to start an rf discharge in a helium vapor using a miniature helical resonator (HNMR in Fig. 1a). The electrons with an average energy of order 100 eV [8] created during the SC discharge bombarded the H_2 films and dissociated a fraction of hydrogen molecules there, thus giving rise to the ESR signals of H atoms in solid H_2. We also used the dissociator for creating a flux of H atoms in the gas phase for calibration of the absolute number of H atoms in the H_2 films we studied [8].

The TU samples of H atoms in solid H_2 films were created similarly with the exception that we did not condense helium gas needed to run the discharge as in TX studies. We made H_2 films by depositing hydrogen gas from the room-temperature gas-handling system onto the quartz microbalance at $T \simeq 0.7$ K. After that, the sample cell was cooled to T=0.1 K and the measurement began. The Turku SC was previously used for our experiments with molecular tritium films [10] and at the time of this measurement only of order 10^{15} tritium atoms remained trapped in the SC walls and mirrors. The electrons released during tritium decay permanently bombarded the films, and dissociated a fraction of H_2 molecules there. This led to a continuous H atom ESR signal buildup. The dissociator in the Turku experiments was used only for filling the SC with the H gas for calibration purposes [2, 8, 21].

In both TX and TU experiments, we used a concentration dependent broadening of H atom ESR lines caused by dipolar interaction between the electron spins of H atoms to estimate the local concentrations of hydrogen atoms in the H_2 films [8, 21]. For TU H in H_2 samples it also allowed us to determine a total number of H atoms in the films since 5.7 keV electrons penetrated through the whole H_2 films and created H atoms there uniformly. 100 eV electrons created in TX studies during the discharge were able to dissociate H_2 molecules only within a thin layer with a thickness of about 100 nm below the sample surface and a separate calibration of the H atom ESR signals was required in order to estimate their total number in H_2 films (see supplemental material of Ref. [2] for more detail).

Sample	Setup	Symbol	Initial composition	Thickness (μm)	E_e (keV)	dn_H/dt ($\times 10^{13}$cm^{-3}s^{-1})
1[2, 23]	TX	●	0.75-o	2.5	~0.1	6
2[2, 23]	TX	◆	0.95-p	0.65	~0.1	5
3[23]	TX	▲	0.97-p	0.2	~0.1	90
4[23]	TX	■	0.998-p	2.5	~0.1	100
5	TU	●	0.75-o	2.5	5.7	1.0
6	TU	●	0.998-p	2.5	5.7	1.7
7	TU	○	0.75-o	2.5	5.7	0.19 (before annealing), 0.30 (after)

Table I. A list of samples and the experimental conditions used in this work.

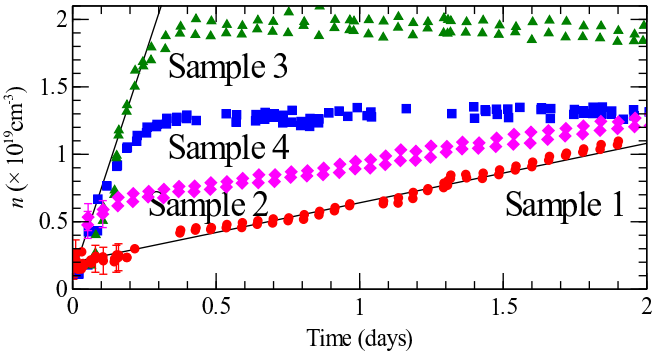

Figure 2. H atom accumulation in 2.5 μm n-H_2 Sample 1 (red circles), 0.95-para H_2 sample Sample 2 (pink diamonds), 0.97-para H_2 Sample 3 (green triangles), and p-H_2 Sample 4 (blue squares) studied in Texas [23]. A larger n-scale offset for Sample 2 (pink diamonds) is due to a higher power used for starting the discharge at t=0. All points shown in the figure were then taken at regular discharge parameters.

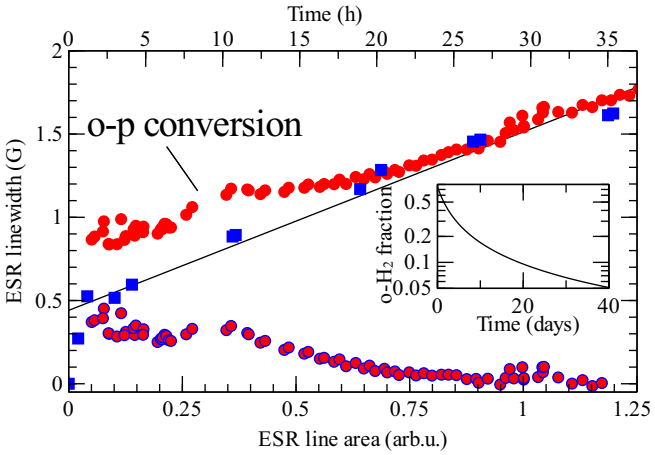

Figure 3. Dependence of H-atom ESR linewidths on ESR line area in n-H_2 sample 1 (red circles) and para-H_2 sample 4 (blue squares) studied in TX. Narrowing of the H atom ESR lines due to the presence of ortho-H_2 molecules as a function of time in Sample 1 is shown with red/blue circles. The time scale is only for Sample 1. Calculated time evolution of ortho-H_2 fraction in normal H_2 due to natural ortho-para conversion without an impact from H atoms is shown in the inset.

III. EXPERIMENTAL RESULTS

In this section, we present the results on the observed production rate of H atoms in the TX and TU samples in the 0.2-2.5 μm H_2 films. The films studied in Texas were also partially described in our previous work on purely spatial diffusion of H atoms [23]. After the deposition, the TX H_2 films were stored at T=0.67 K and the rf discharge was run continuously over a period of about 3 weeks. TX Sample 1 was made of normal H_2 gas (75% ortho, 25% para) (red circles in Fig. 2), while Sample 2 was prepared from H_2 stored in the dissociator chamber for about 30 days (pink diamonds in Fig. 2). We use an o-H_2 and p-H_2 notation for ortho-H_2 and para-H_2 throughout the article. Based on the rate of natural ortho-para conversion in solid H_2 (1.9%/h) [29], we estimate that the o-H_2 fraction in this film at the moment of film deposition was ≃5%. Sample 3 (green triangles in Fig. 2) was stored in the dissociator for 2 months and expected to have ≃3% of o-H_2 right after film deposition. Sample 4 (blue squares in Fig. 2) was made of H_2 converted in an ortho-para converter and expected to contain only≃ 0.2% o-H_2.

The scatter of data shown in Fig.2 at t=0 is a result of the low ESR signal-to-noise ratio right after starting the discharge. This leads to errors of determining H atom concentration. Also, for starting the discharge for Sample 2, it was necessary to supply a larger rf power as compared with the other three samples. This led to a larger offset of H atom concentration for this sample at t=0. After starting the discharge at a higher power level, the discharge power was adjusted to be similar to that used for other three samples.

For these TX samples, we observed a nearly one order of magnitude more efficient accumulation of H atoms in mostly para-H_2 Samples 3 and 4 containing 0.2-3% of o-H_2 at the beginning of running the discharge as compared with the films made of ~5-75% ortho H_2 (Samples 1 and 2). We observed that in TX Sample 4, the H atom ESR line broadening caused by the presence of o-H_2 molecules nearly completely vanished within the first 24 hours of running the discharge (Fig. 3). Despite different accumulation rates in the TX samples, the equilibrium concentrations of H atoms in all these films were

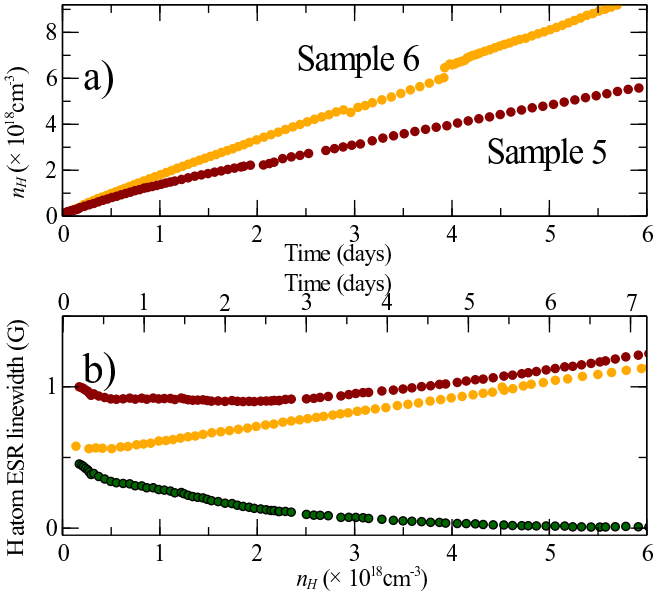

Figure 4. a) H atom accumulation in TU 2.5 μm n-H_2 Sample 5 (brown circles) and 2.5 μm thick p-H_2 Sample 6 (orange circles). b) Dependence of H atom linewidth on concentration in n-H_2 (brown circles) and p-H_2 TU samples (orange circles). Broadening of the H atom ESR lines due to the presence of ortho-H_2 molecules varying inversely as a function of time in Sample 5 is shown by green circles. The time scale is only for the n-H_2 sample.

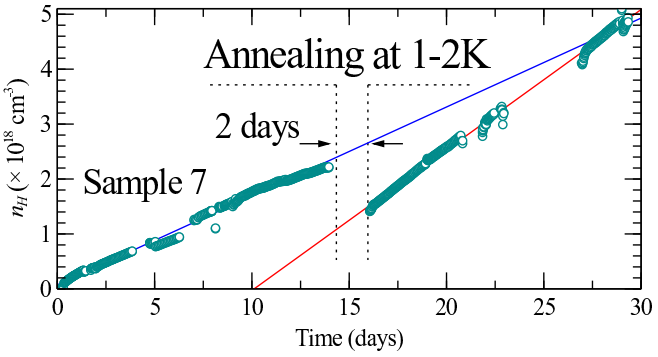

Figure 5. H atom accumulation rate before and after annealing at 1-2K in the 2.5 μm n-H_2 TU Sample 7.

nearly the same, $\simeq$1-2$\times10^{19}$cm^{-3}. These concentrations were reached within less than half a day for samples 3 and 4 and within about 2 days for samples 1 and 2 (see Fig. 2). The saturation of concentration is determined by an equilibrium between the rate of atom production and their recombination [2, 23].

We carried out a similar set of experiments in Turku where H_2 films with different initial o-p contents were exposed to a flux of 5.7 keV electrons emitted during tritium decay. We studied H atom accumulation in 2.5 μm thick H_2 films made from n-H_2 gas (Sample 5) and p-H_2 gas (Sample 6) prepared in an ortho-to-para converter for about 24 hours. The films were deposited directly from the room temperature gas-handling system at the deposition rate of 0.1-1 monolayers/s. After the film deposition, we stabilized the SC temperature at 0.1 K and monitored the H atom ESR signal evolution over a time period of several weeks.

In these studies, we observed a slower accumulation rate, dn_H/dt, of H atoms as compared with the TX studies (see Table I). However, comparing the absolute accumulation rates in TU and TX experiments in terms of concentration growth in the samples cannot be done due to the difference in mechanisms of creating atoms, i.e. thicknesses of layers where they are created either by the 100 eV or 5.7 keV electrons, respectively. Faster concentration growth in TX samples is a consequence of the much thinner layer where the atoms are generated while the rate in terms of the total number of atoms dN/dt in the sample may be even smaller than that in Turku. This also concerns the maximum achieved concentrations. It is seen from the plots in Fig. 2 and Fig. 4 that the accumulation process is saturated for low o-H_2 TX samples within few hours after starting the discharge. For the o-H_2 rich TX samples, this was reached after 2-3 days (Fig. 2 and Fig. 5 of ref. [23]), and for the TU samples the accumulation is not saturated even after 6 days of observation. So, the maximum concentrations for the TU samples under study of this work were not reached and may be much higher than those in Texas. In our previous work [10], we used much larger amounts of tritium which had been mixed with H_2 in the films. Maximum concentrations of 2×10^{20}cm^{-3} were reached, limited by thermal explosions of the samples. Despite this difference in the H production mechanism, in TU samples we also observed faster H atom accumulation in Sample 6 with a low o-H_2 concentration as compared with n-H_2 Sample 5. The effect, however, was smaller (see Table I) than that observed in TX samples (Fig. 4). The accumulation rate difference between the two TU samples was about 70%. We observed that o-p conversion in the vicinity of H atoms in TU Sample 5 took place much slower as compared with TX Sample 1 (see Fig. 3 upper time scale). The o-H_2 contribution to H atom ESR line broadening was observed up to about five days of sample storage (Fig. 4b). Similar to TX samples, the accumulation rate did not change with time whereas ortho-para conversion should have changed the percentage of ortho and para fractions in the H_2 films.

In addition to that, we also studied the influence of sample annealing on the H atom accumulation rate in TU Sample 7. This sample was studied after a long summer break where the setup was warmed up to room temperature and the SC was evacuated to high vacuum thus reducing the number of trapped T atoms in the sample cell walls and the accumulation rate of H atoms in Sample 7. First, we created a 2.5 μm H_2 film made from normal H_2 gas and stored it for 14 days at T=0.1 K. After that, we gradually increased the SC temperature to carry out film annealing at temperatures 1-2 K for about 2 days. We did not increase the SC temperature above

2 K in order to avoid H_2 film sublimation which might influence the observed accumulation rate. We monitored the H_2 film thickness during annealing by the quartz microbalance and concluded that the film thickness did not change. At the same time, the H atom concentration after annealing decreased almost by a factor of two. After the film was annealed, we cooled the SC back to T=0.1 K and continued to measure H atom signal evolution at this temperature. We observed that the H atom accumulation rate after the film annealing increased by about 60% (Table I) and remained unchanged over the next 3 weeks of sample accumulation. We also verified that the accumulation rate increase was not related to the spectrometer sensitivity change or other instrumental effects. The results of this measurement are presented in Fig. 5.

IV. DISCUSSION

In this work, we presented our results on accumulation of H atoms in different solid H_2 films with a thickness of 0.2-2.5 μm. The samples were studied in two different setups in Turku and Texas and the H atom accumulation was carried out via the H_2 film bombardment by electrons produced during tritium decay and running the rf discharge, respectively.

For TX samples, we observed that the H atom accumulation takes place much faster in the films made of H_2 gas with small content of ortho-H_2 (0.2-3%) as compared with the samples made of n-H_2. A similar although less pronounced behavior was also observed in TU samples where electrons used for bombarding H_2 films created during tritium decay have average energy of 5.7 keV as compared with $\simeq$0.1 keV electrons in the TX studies.

We consider different ortho-para content and the H_2 film structure as the possible reasons for the observed faster H atom accumulation in p-H_2 films. First, we discuss the possible importance of the film ortho-para composition. We studied films with different ortho-para content: both of the films made from H_2 with a normal o-p composition and para-H_2 films with a small ortho admixture of $\simeq$0.2-3%.

In both experiments, we were able to track ortho-para conversion of H_2 molecules at the initial stage of accumulation by monitoring the H atom ESR line broadening caused by the presence of o-H_2 molecules in the films. The presence of H atoms greatly stimulated o-p conversion in both types of samples. The rate of o-p conversion in n-H_2 films for these two samples is defined by the local concentration of H atoms and their diffusion rate in the H_2 matrix. The studies of diffusion of ^{3}He atoms in solid ^{4}He revealed an inverse dependence of the ^{3}He atom diffusion rate on their concentration [30]. As a result, the o-p conversion time should be inversely proportional to H atom concentration in the absence of H atom diffusion, but a deviation from this dependence should be observed if the H atom diffusion stimulates conversion.

In Sample 1, ortho-para conversion reduced the o-H_2 broadening of H atom ESR lines by a factor of 2 within about 15 h (red-blue circles in Fig. 3) at the corresponding H atom concentration of $\simeq 5\times10^{18}$cm^{-3} (Fig. 2). A factor of 2 reduction of o-H_2 broadening in TU Sample 5 (green circles in Fig. 4) took place in about 1.5 days for an H atom concentration of 1.3×10^{18}cm^{-3}. This indicates no clear enhancement of o-H_2 conversion rate in the TU Sample 5 as compared to TX Sample 1 where H atom diffusion in solid H_2 films is expected to be faster due to a smaller H atom concentration. This may indicate a preferential diffusion of H atoms only in the regions of TU Sample 5 rich in p-H_2. Such behavior was also described by Shevtsov et al. [31] who attempted to measure the rate of pure H atom spatial diffusion in n-H_2 films by measuring the rate of o-p conversion in n-H_2 films. We, however, did not observe any accumulation rate enhancement during stimulated o-p conversion in either TX or TU samples. The accumulation rates did not change upon sample storage, even though ortho-H_2 content in these samples decreased significantly. We, thus, conclude that the change of ortho-para content in the films due to interaction with H atoms during accumulation does not influence the H atom accumulation rates.

The H atom accumulation rate may, however, depend on the H_2 film structure defined by the *initial* ortho-para composition. Such a dependence may come from a different lattice type or different number of lattice defects for ortho-H_2 and para-H_2 rich samples created during the film deposition. Quench-condensed films deposited onto a cold substrate at T=1-1.5 K are expected to be uniform but may have some short-scale defects and structural disorder. Local defects may serve as centers where a pair of two H atoms created during an H_2 molecule dissociation recombine. The studies of thin H_2 film specific heats showed a broader $C_{H_2}(T)$ peak for n-H_2 films as compared with bulk n-H_2 samples which was attributed to the H_2 film defects [32]. We probed the influence of film defects on accumulation rate by H_2 film annealing. We observed a more efficient H atom production in a TU sample where the accumulation rate noticeably increased after annealing the H_2 film at T=1-2 K as shown in Fig. 5.

One of the interesting observations is a qualitatively similar behavior of n-H_2 Sample 1 and 95%-para H_2 Sample 2. Kumada et al. [11] found a maximum of H atom recombination rate in solid H_2 at the initial o-H_2 concentration of about 10%. This can qualitatively explain a similarity of the behavior of H atoms in both normal H_2 Sample 1 and 95%-para H_2 Sample 2. A future more detailed study of H atom accumulation rate in the crossover region of othro-H_2 content of a 1-10% can provide further insight into understanding of this behavior.

Another interesting observation is a much smaller difference of H atom accumulation rates for p-H_2 and n-H_2 films studied in Turku as compared with those in TX. The observed accumulation rate difference for the TU samples was about 70% even though it was nearly an order of magnitude (1000%) for the TX samples. We speculate that different mechanisms for H atom produc-

tion in these samples may explain such a large difference. The H atom production in the TX samples where electrons have energies of about 0.1 keV mostly takes place through a direct dissociation of H_2 molecules by electron impact: H_2=H+H. For the TU samples exposed to more energetic 5.7 keV electrons, H_2 molecule ionization with a formation of H_2^+ ions is the most probable process. The H_2^+ ions then rapidly react with the neighboring H_2 molecules via reaction H_2^++H_2=H_3^++H. We did not find in the literature evidence for the dependence of H_2 molecule ionization cross-section on the H_2 molecule rotational state. We, therefore, consider that only one atom per ionization event is produced for both n-H_2 and p-H_2 films. Since H atoms in TX samples are generated in pairs, they can be trapped by the lattice defects and recombine back to molecules right after dissociation. This process might be more efficient in ortho-H_2 rich samples. In TU samples, H_2^++H_2=H_3^++H reaction produces single atoms which do not recombine until they diffuse to another H atom.

The H_3^+ ions can then recombine with electrons and produce three H atoms. The H_3^+ ion and electron concentrations should be of order of that for free H atoms ($\simeq$0.01%), and thus this mechanism of H atom production should be less efficient than ionization with a subsequent H_2^++H_2=H_3^++H reaction.

The observed difference of 70% for the accumulation of the Turku samples as compared with a much larger effect for the TX samples might be attributed to the production of H atoms by a different mechanism, namely direct dissociation of H_2 molecules similar to that taking place in TX samples. This direct dissociation in TU samples can be attributed to lower energy electrons in the tritium decay spectrum or electrons decelerated after collisions with the sample cell walls or H_2 molecules in the film. These H atom pairs can recombine at the lattice defects and thus be susceptible to the initial o-p composition of the H_2 film. This can take place for low-energy electrons in the tritium beta-particle spectrum or electrons which lose their energy due to collisions with H_2 molecules or samples cell walls.

V. CONCLUSION

In conclusion, we studied the H atom accumulation in normal and para-H_2 films in two kinds of solid 0.2-2.5 μm H_2 films: H_2 films exposed to low energy ($\simeq$0.1 keV) electrons produced during the rf discharge (Texas samples) and those bombarded by 5.7 keV electron generated during tritium decay (Turku samples). We observed a faster H atom accumulation in para-H_2 films for both types of samples. This difference was about an order of magnitude for the Texas samples and only 70% for the films studied in Turku. We suggest that the accumulation rate difference for normal and para-H_2 samples can be attributed to different initial structure of these H_2 samples and a possibly higher number of film defects in ortho-H_2 rich samples. A smaller difference in the accumulation rates between normal and para-H_2 seen for the samples for Turku and Texas samples can be caused by different H atom production mechanisms: a direct dissociation of H_2 molecules and their ionization with a subsequent reaction of H_2^+ ions with neighboring H_2 molecules for Turku samples versus a direct dissociation with a production of two H atoms for TX samples.

ACKNOWLEDGMENTS

This work has been supported by NSF Grant No. DMR 2104756 and Academy of Finland Grant No. 317141.

[1] D. Zhou, C. M. Edwards, and N. S. Sullivan, Phys. Rev. Lett. **62**, 1528 (1989).
[2] S. Sheludiakov, D. M. Lee, V. V. Khmelenko, J. Järvinen, J. Ahokas, and S. Vasiliev, Phys. Rev. Lett. **126**, 195301 (2021).
[3] Y. A. Dmitriev, Physica B: Condensed Matter **392**, 58 (2007).
[4] Y. A. Dmitriev, J. Low Temp. Phys. **180**, 284 (2015).
[5] E. B. Gordon, A. A. Pel'menev, O. F. Pugachev, and V. V. Khmelenko, JETP Lett. **37**, 282 (1983).
[6] S. I. Kiselev, V. V. Khmelenko, and D. M. Lee, Phys. Rev. Lett. **89**, 175301 (2002).
[7] J. Ahokas, J. Järvinen, V. V. Khmelenko, D. M. Lee, and S. Vasiliev, Phys. Rev. Lett. **97**, 095301 (2006).
[8] J. Ahokas, O. Vainio, S. Novotny, J. Järvinen, V. V. Khmelenko, D. M. Lee, and S. Vasiliev, Phys. Rev. B **81**, 104516 (2010).
[9] G. W. Collins, P. C. Souers, J. L. Maienschein, E. R. Mapoles, and J. R. Gaines, Phys. Rev. B **45**, 549 (1992).
[10] S. Sheludiakov, J. Ahokas, J. Järvinen, L. Lehtonen, O. Vainio, S. Vasiliev, D. M. Lee, and V. V. Khmelenko, Phys. Chem. Chem. Phys. **19**, 2834 (2017).
[11] T. Kumada, M. Sakakibara, T. Nagasaka, H. Fukuta, J. Kumagai, and T. Miyazaki, J. Chem. Phys. **116**, 1109 (2002).
[12] T. Kumada, J. Chem. Phys. **124**, 094504 (2006).
[13] J. Eloranta, K. Vaskonen, and H. Kunttu, J. Chem. Phys. **110**, 7917 (1999).
[14] M. E. Balabanoff, M. Ruzi, and D. T. Anderson, Phys. Chem. Chem. Phys. **20**, 422 (2018).
[15] A. I. Strom, K. L. Fillmore, and D. T. Anderson, Low Temp. Phys. **45**, 676 (2019).
[16] F. M. Mutunga, K. M. Olenyik, A. I. Strom, and D. T. Anderson, J Chem. Phys. **154**, 014302 (2021).
[17] P. Souers, *Hydrogen Properties for Fusion Energy* (University of California Press, 1986).
[18] C.-Y. Kuo, R. J. Kerl, N. D. Patel, and C. K. N. Patel, Phys. Rev. Lett. **53**, 2575 (1984).

[19] M. D. Correnti, K. P. Dickert, M. A. Pittman, J. W. Felmly, J. J. I. Banisaukas, and L. B. Knight Jr., J. Chem. Phys. **137**, 204308 (2012).
[20] B. Zhou, B. Yang, N. Balakrishnan, B. K. Kendrick, M. Chen, and P. C. Stancil, Mon. Not. R. Astron. Soc. **507**, 6012 (2021).
[21] J. Ahokas, O. Vainio, J. Järvinen, V. V. Khmelenko, D. M. Lee, and S. Vasiliev, Phys. Rev. B **79**, 220505(R) (2009).
[22] S. Sheludiakov, J. Ahokas, J. Järvinen, D. Zvezdov, O. Vainio, L. Lehtonen, S. Vasiliev, S. Mao, V. V. Khmelenko, and D. M. Lee, Phys. Rev. Lett. **113**, 265303 (2014).
[23] S. Sheludiakov, D. M. Lee, V. V. Khmelenko, Y. A. Dmitriev, J. Järvinen, J. Ahokas, and S. Vasiliev, Phys. Rev. B **105**, 144102 (2022).
[24] S. Sheludiakov, J. Ahokas, J. Järvinen, L. Lehtonen, S. Vasiliev, Y. A. Dmitriev, D. M. Lee, and V. V. Khmelenko, Phys. Rev. B **97**, 104108 (2018).
[25] S. Sheludiakov, D. M. Lee, V. V. Khmelenko, J. Ahokas, J. Järvinen, and S. Vasiliev, J. Low Temp. Phys. **208**, 67 (2022).
[26] S. Sheludiakov, J. Ahokas, O. Vainio, J. Järvinen, D. Zvezdov, S. Vasiliev, V. V. Khmelenko, S. Mao, and D. M. Lee, Rev. Sci. Instrum. **85**, 053902 (2014).
[27] S. Sheludiakov, D. M. Lee, V. V. Khmelenko, J. Järvinen, J. Ahokas, and S. Vasiliev, Rev. Sci. Instrum. **91**, 063901 (2020).
[28] S. Vasilyev, J. Järvinen, E. Tjukanoff, A. Kharitonov, and S. Jaakkola, Rev. Sci. Instrum. **75**, 94 (2004).
[29] I. F. Silvera, Rev. Mod. Phys. **52**, 393 (1980).
[30] V. N. Grigor'ev, Low Temp. Phys. **23**, 3 (1997).
[31] V. Shevtsov, A. Frolov, I. Lukashevich, E. Ylinen, P. Malmi, and M. Punkkinen, J. Low Temp. Phys. **95**, 815 (1994).
[32] J. Birmingham, P. Richards, and H. Meyer, J. Low Temp. Phys. **103**, 183 (1996).